

# A Review on Modelling of the Maximum Lagging Current Test Method of Salient Pole Synchronous Machines

A. Darabi\*<sup>(C.A.)</sup>, M. Yousefifefat\* and M. Nikkhoo\*

**Abstract:** Quadrature-axis reactance for various reasons comes into account as one of the most important parameters of salient pole synchronous machine. There are several common standard methods for measuring this parameter that also have been explained with some details in the standards, scientific papers and text books. One of these methods is the maximum lagging current test that is done simply at no-load, having a three phase voltage source and applying very low power even for a high power machine. How this experiment is done is described at some references such as the books related to electrical machinery. This paper presents a detail analysis and description of the test and some simulation results regarding the performance of the machine during pole-slipping. It is shown when the reversal field current is increased very slowly, the transient of the pole-slipping commences at load angle equal to 45 degrees or by a better language at 225 instead of zero which is the common opinion of almost all the previously published literatures. In this paper, a realistically developed analysis of the test is presented applying appropriate assumptions. The maximum lagging current test is then simulated applying a small salient pole machine with the rated 31.5 kVA using MATLAB/SIMULINK. Some simulation results are illustrated that prove correctness and validity of the new analysis and the proof described by the present paper.

**Keywords:** Maximum Lagging Current Test, Quadrature-axis Reactance, Salient Pole Synchronous Machine Parameters.

## 1 Introduction

Synchronous machine as one of the most important elements of power systems plays an essential role in producing electrical energy. These machines have a set of circuit parameters [1, 2] which computing their accurate values are very important while designing a machine with predefined desirable operation. Due to existing uncertainty in the analytical method, measuring of the parameters is much essential after manufacturing in order to prepare the data sheet and the instruction manual of the machine. These parameters are required for almost all simulations predicting the steady state, dynamic transient, performing stability studies and post mortem analyses of failures [3-8].

Nowadays, electromagnetic circuit based analytical methods, numerical methods such as finite elements (FE) and the techniques based on experiments are three main methods to achieve the parameters of the electrical

equivalent circuit of the machines [9]. Among them there are many different off-line test methods evaluating the circuit parameters of the salient pole synchronous machine that have been discussed in the books, valuable papers and particularly in the standards such as [10, 11]. The quadrature-axis reactance of the salient pole machines is an important parameter differentiating the salient pole machines from cylindrical ones. Also, three common experimental methods have been presented in the text books for measuring this parameter known as slip test, reluctance motor test and the maximum lagging current test [10]. Generally, the maximum lagging current test of a synchronous machine is carried out at the no-load motor operating mode using a three phase voltage source with the frequency equal to rated frequency and the amplitude a bit lower than the nominal voltage of the machine. The motor runs with the nominal synchronous speed requiring a very low power and for this reason the maximum lagging current test becomes very important and rather different from two other methods. Therefore the maximum lagging current test is one of the most common and convenient ways of measuring parameter of small, medium and even very large salient pole synchronous machines. As

---

Iranian Journal of Electrical & Electronic Engineering, 2014.

Paper first received 7 July 2013 and accepted 3 Dec. 2013.

\* The authors are with the Faculty of Electrical & Robotic Eng., University of Shahrood, Shahrood, Iran.

E-mails: darabi\_ahmad@hotmail.com, m.yousefi398@gmail.com and m.nikkhoo@hotmail.com.

mentioned earlier, except in particular cases that the value of is very small, the voltage of the power supply for the maximum lagging current test is chosen quite close to the nominal values. In fact, the voltage of power supply must be chosen in a way that the current of the machine during the maximum lagging current test not to exceed much from the rated value. However, since the values of depending on the size and design are not the same for different machines and there is no trustworthy way of the value prediction before measurement, it is recommended that the voltage is adjusted to a value less than 75% of the nominal voltage of the test machine [10]. Among the text books, the one written by Professor Bimbhra completely describes the maximum lagging current test method [12]. This book firstly presents a proper way of doing the test and gives a correct formula for calculating and then it tries to give a proof for the formula of calculation by an example. It seems that assumptions and arguments given as a proof for the test formula by [12] not to be right as will be discussed by the present paper. Moreover, some new papers such as [13] have used the results of the maximum lagging current test from reference [12, 14] that it seems not pay enough attention to analyses of test. This paper firstly explains the incorrect assumptions and proving given by the above mentioned book for the maximum lagging current test and then an acceptable proof is presented by employing the correct assumptions. For further assurance regarding the claiming proof of the present paper, a numerical simulation of the maximum lagging current test is carried out using a 4-pole, Y connection, salient pole synchronous machine with the rated values of 31.5 kVA, 50 Hz and 400 volts made by Leroy Somer Ltd. Detailed information about the circuit parameters of the machine have been already evaluated using FE and given by [15, 16]. These parameters are used in a MATLAB/SIMULINK simulation and a few simulation results are illustrated. All the results presented in this paper show the deficiencies of the proving given by the previous publications and confirm the claiming proof of the present paper for the maximum lagging current test. Therefore, the authors of the present paper believe that the new proof should be applied instead of existing proof in the future editions of the text books with some confidences.

## 2 The Maximum Lagging Current Test Method

In the maximum lagging current test, firstly the salient pole test machine is started-up by a prime mover to operate with the nominal speed. The synchronism operation of the three phase synchronous machine with the artificial main is then created by applying an appropriate current into the field winding and connecting the terminals of the machine to the output terminals of an autotransformer fed by the grid. The reason for employing the autotransformer is to provide somewhat reduced voltage for the test machine such that

the current of the machine remains within the rated values during the maximum lagging current test. After constructing a synchronism operation, the prime mover can be turned off and let the salient-pole synchronous motor continue working at the no-load conditions. Now the machine is ready to be put in the maximum lagging current test. In order to perform the test, firstly the field current is reduced gradually until it reaches to zero eventually. At the last point, back emf becomes zero. By ignoring the armature winding resistance, the following equation shows per-phase power of the motor:

$$P = \frac{E_f V_t}{X_d} \sin(\delta) + \frac{V_t^2}{2} \left( \frac{1}{X_q} - \frac{1}{X_d} \right) \sin(2\delta) \quad (1)$$

where,  $P$  is per phase of Electromagnetic power in the air gap,  $V_t$  is rms per phase terminal voltage,  $E_f$  is rms per phase back emf,  $\delta$  is power angle and  $X_d$  is direct-axis synchronous reactance.

The first part of the Eq. (1) is the electromagnetic power that the value would be zero when the excitation becomes zero. The second part of the equation belongs to the reluctance power produced by the saliency of the poles. The reluctance power always has a non-zero value except at  $\delta = 0$  deg so, when the field current becomes zero, a no-load salient pole synchronous motor continues to operate as a reluctance motor with a small  $\delta$  value to overcome the friction load at synchronous speed. The next step of the maximum lagging current test is to reverse the field current using the appropriate switch. Reversed field current is then slowly increased from zero until a short while out of synchronism or pole slipping happens. For the time duration beginning from the moment of filed reversal until the time before pole slipping, the only running torque is the reluctance torque. In this situation, electromagnetic or interaction torque similar to the load acts against the driving reluctance torque. On the other hand, due to negative field current, the lagging armature current and reactive power increase greatly to compensate shortage of the excitation and thus to keep the air gap flux constant corresponding to the terminal voltage. In the maximum lagging current test as mentioned earlier in a certain value of reversal field current, the rotor suddenly loses its synchronism for a limited time. Hence after slipping a rotor pole, motor will be back to synchronism again. Phase voltage ( $V_t$ ) and current ( $I_a$ ) of the machine are recorded just for the instant before slipping the poles. Using the values of these quantities, the reactance of the quadrature-axis is then evaluated using:

$$X_q = \frac{V_t}{I_a} \quad (2)$$

The advantage of the maximum lagging current test is that the value of  $X_q$  is measured at nearly normal saturated operating conditions. Anyway for a specific synchronous machine with a big value of  $X_d$  to  $X_q$

ratio or a large value of the armature current, the maximum lagging current test might be accomplished applying a lower voltage [12].

### 3 Analysis and Proving the Maximum Lagging Current Test

This section is devoted to proving the maximum lagging current test method of  $X_q$  parameter measurement that its final result has been represented in Eq. (2). Let us divide this section into two subsections. In the first subsection, we review and discuss the analysis and proof given by a few previously published references emphasizing on reference [12] which considers this topic with much details. In the second part, it is proven that perceptive of the machine operation during the maximum lagging current test and thus assumptions applied by the previous literatures are quite far from the experiment conditions. Thereafter, a correct proof for the Eq. (2) is given in this section applying appropriate realistic assumptions in agreement with the machine operation.

#### 3.1 Common Proving Represented in the Previous Publications

Reference [12] analyses the performance of the salient pole synchronous machine during the maximum lagging current test and then presents the solution of example 5-40 as a proof of the Eq. (2). The armature winding resistance and rotational losses of the machine are assumed negligible while formulating the maximum lagging current test. The author applies these assumptions and concludes that both the power angle and active power taken from the power supply are equal to zero. Therefore the phasor diagram shown in Fig. 1 can be used during the maximum lagging current test for any values of the field current before pole slipping to represent the proof given in reference [12]. According to this figure, power angle always is equal to zero and  $\bar{E}_{f1}, \bar{E}_{f2}, \dots, \bar{E}_f$  which are the phasors of the back emf or open circuited voltage for various field currents are drawn along with the terminal voltage shown by  $\bar{V}_t$ .

Now for any synchronous operation of the motor with a negative field current, active and reactive input motor power can be calculated respectively as follows:

$$P = -\frac{E_f V_t}{X_d} \sin \delta + \frac{V_t^2}{2} \left( \frac{1}{X_q} - \frac{1}{X_d} \right) \sin 2\delta \quad (3)$$

$$Q = \frac{E_f V_t}{X_d} \cos \delta + \frac{V_t^2}{X_d} + V_t^2 \left( \frac{1}{X_q} - \frac{1}{X_d} \right) \sin^2 \delta \quad (4)$$

As mentioned earlier when the reversal field current of the motor is increased gradually, pole slipping happens at a particular value of the field current. However, according to the assertion of reference [12], for the value of the negative field current in which the out of synchronism occurs, we have:

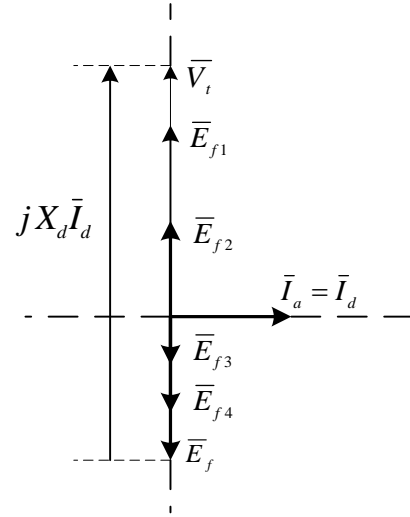


Fig. 1 Phasor diagram of the synchronous motor in the maximum lagging current test (Based on presentation of [12]).

$$\frac{dP}{d\delta} = 0 \quad (5)$$

Therefore:

$$\frac{dP}{d\delta} = -\frac{E_f V_t}{X_d} \cos(\delta) + V_t^2 \left( \frac{1}{X_q} - \frac{1}{X_d} \right) \cos(2\delta) = 0 \quad (6)$$

On the other hand with respect to Fig. 4, pole slipping occurs at  $\delta = 0$  deg so:

$$\frac{dP}{d\delta} = -\frac{E_f V_t}{X_d} + V_t^2 \left( \frac{1}{X_q} - \frac{1}{X_d} \right) = 0 \quad (7)$$

Consequently, the back emf at the moment of pole slipping will be:

$$E_f = V_t \left( \frac{X_d}{X_q} - 1 \right) \quad (8)$$

Moreover, since in this situation, the loss free motor is operating at no load, the input power and lagging angle will be zero and  $\varphi = 90$  deg respectively. Therefore the reactive power can be written as:

$$Q = V_t I_a \sin \varphi = V_t I_a \quad (9)$$

According to Eq. (4) and Eq. (9), and assuming  $\delta = 0$  deg we have:

$$Q = V_t I_a = \frac{E_f V_t}{X_d} + \frac{V_t^2}{X_d} \quad (10-a)$$

or:

$$Q = \frac{V_t}{X_d} (E_f + V_t) \quad (10-b)$$

where,  $Q$  is per phase input reactive power. Therefore:

$$I_a = \frac{1}{X_d} (E_f + V_t) \quad (11)$$

Finally by substituting  $\bar{E}_f$  from Eq. (8) into Eq. (11) we will have:

$$I_a = \frac{1}{X_d} [V_t (\frac{X_d}{X_q} - 1) + V_t] = \frac{V_t}{X_q} \quad (12)$$

or:

$$X_q = \frac{V_t}{I_a} \quad (13)$$

Therefore the final formula for the maximum lagging current test given as Eq. (2), is obtained.

### 3.2 Analysis and Proving Given by the Present Paper

Obviously, the maximum lagging current test is a practical method for measuring the parameter  $X_q$  of the salient pole synchronous machines. Therefore the hypothesis or argument hired must explain and be consistent with the real occurrences of the experiment. First of all let us look at the input power of the machine during the test. The input active power of machine is assumed to be absolute zero in section 3.1 by ignoring the no-load rotational losses. However, due to existing rotational losses even as a very small and negligible amount, the machine takes some energy from the power source to compensate for the losses. Otherwise pole slipping never happens during the maximum lagging current test. Therefore, it is utterly obligatory to assume the torque of the rotational loss equal to negative zero instead of absolute zero which the later is applied in somewhere of reference [12]. In the present paper, the value of the loss relevant torque is indicated by negative zero to imply a load.

Eq. (1) represents active power of the machine that consists of two components i.e. electromagnetic power and reluctance power. During the operation with any positive field current, both of the power components are positive and act against the losses which the power value is assumed to be very small or negative zero. In this operating condition, the  $\delta$  angle will have a non-zero value depending on the amount of rotational losses and positive field excitation. Any way changing the direction of the field current, alters the sign of the electromagnetic torque from positive to negative so that the electromagnetic torque acts similar to the load against the driving reluctance torque. In this operating condition, any increase of the reversal field current yields to a similar increase of the electromagnetic torque. Therefore the reluctance torque increases likewise to keep the machine operating in synchronous speed. By increasing the reversal field current slowly, the value of  $\delta$  and so the reluctance torque increases correspondingly until the reluctance torque becomes maximum at nearly  $\delta = 225$  deg. After that, the driving reluctance torque reduces by small augment of the negative excitation while the opposing electromagnetic torque increases so the machine loses its synchronism suddenly for a short time. During out of synchronous operating condition the speed of the rotor reduces until a pole slipping helps to restore the common synchronism

operation. In the new synchronism conditions, both electromagnetic and reluctance torques (or powers) purchase small positive values to respond the loss torque (or power) demand.

Let us here to forget the rest of our discussion shortly and come back to the proving of reference [12] given in section 3.1 where the values of the active power and power angle were assumed zeros for the whole synchronous operation period of the test including the time just before the pole slipping. Nevertheless in the circumstances that the active power and power angle were assumed remaining unchanged, it could not be permitted to apply Eq. (5). Correspondingly the Eq. (8), which was extracted directly from the Eq. (5), is not to be trusted.

Now, the proving of maximum lagging current test of the present paper is followed by a negative zero value assumption of the loss relevant torque. By this assumption, the phasor diagram illustrated by Fig. 2 instead of Fig. 1 can be applied for different values of positive and negative field current during the maximum lagging current test of a salient pole synchronous motor.

In Fig. 2, each phasor of the back emf shown by  $\bar{E}_{fj}$  for  $j = 1, 2, \dots$  corresponds with a particular value of the field current.

It would be preferable to describe the active and reactive powers of the machine as their initial forms regardless of the sign of the field current as follows:

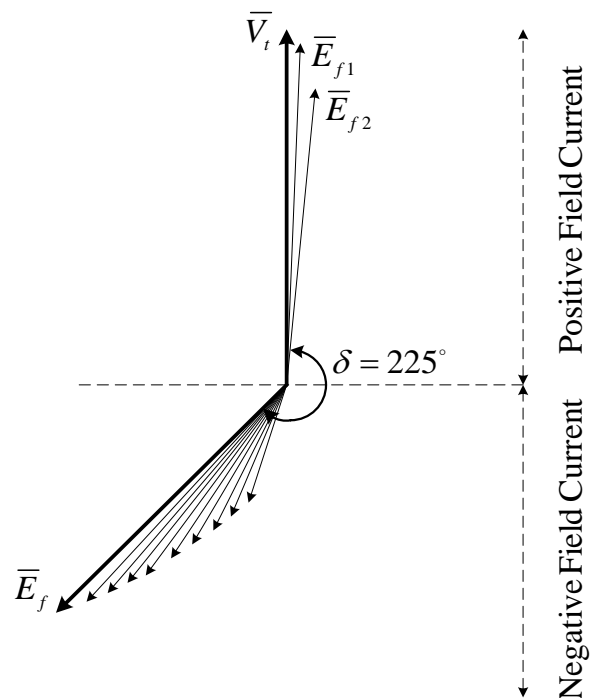


**Fig. 2** Phasor diagram of the salient pole synchronous motors for the maximum lagging current test (Based on presentation of the current paper).

$$P = \frac{E_f V_t}{X_d} \sin(\delta) + \frac{V_t^2}{2} \left( \frac{1}{X_q} - \frac{1}{X_d} \right) \sin(2\delta) \quad (14)$$

$$Q = -\frac{E_f V_t}{X_d} \cos(\delta) + \frac{V_t^2}{X_d} + V_t^2 \left( \frac{1}{X_q} - \frac{1}{X_d} \right) \sin^2(\delta) \quad (15)$$

in which the values of the parameters behind the sinusoidal terms will be positive in all circumstances but the value of  $\delta$  varies from nearly zero for the positive field currents to about 225 deg for the reversed field current associated with pole slipping as demonstrate visibly in Fig. 2.

During the maximum lagging current test and for all synchronous operations of the machine we have:

$$P = \frac{E_f V_t}{X_d} \sin(\delta) + \frac{V_t^2}{2} \left( \frac{1}{X_q} - \frac{1}{X_d} \right) \sin(2\delta) \approx 0 \quad (16)$$

On the other hand since in the maximum lagging current test, the maximum reluctance torque and consequent loss of synchronism operation occur at  $\delta = 225$  deg, the value of corresponding back emf can be evaluated by substituting  $\delta = 225$  deg into Eq. (16) as follows:

$$E_f = \frac{V_t}{\sqrt{2}} \left( \frac{X_d}{X_q} - 1 \right) \quad (17)$$

This equation is different from Eq. (8) by a factor of  $\sqrt{2}$  where it can be simply applied experimentally to consider the validation of the new proving approach.

Now by considering approximately no-load condition, power factor and  $\delta$  for the instant just before loss of synchronization will be almost equal to zero and 225 deg respectively. Therefore according to Eq. (4), the reactive power at this moment will be as follows:

$$\begin{aligned} Q = V_t I_a &= \frac{E_f V_t}{\sqrt{2} X_d} + \frac{V_t^2}{X_d} + \frac{V_t^2}{2} \left( \frac{1}{X_q} - \frac{1}{X_d} \right) \\ &= \frac{E_f V_t}{\sqrt{2} X_d} + \frac{V_t^2}{2} \left( \frac{1}{X_q} + \frac{1}{X_d} \right) \end{aligned} \quad (18)$$

By substituting Eq. (17) into Eq. (18), the final equation of maximum lagging current test will be achieved which have been already denoted by Eq. (2).

In the present proof, the phasor diagram of the synchronous motor for the time exactly before loss of synchronism would be as shown in Fig. 3. According to Fig. 3, one can write:

$$X_d I_d = E_f + \frac{V_t}{\sqrt{2}} \quad (19)$$

Eq. (2) can be obtained again by substituting Eq. (17) into Eq. (19) and regarding the Fig. 3 in which  $I_d = I_q = I_a / \sqrt{2}$ .

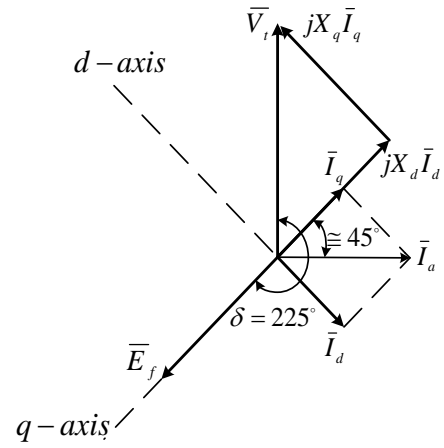


**Fig. 3** Phasor diagram of synchronous motor for the moment just before slipping the poles (Based on presentation of the current paper).

It is noteworthy that the minimum negative excitation required to push the machine in pole slipping operation is related to the terminal voltage and values of  $X_d$  and  $X_q$  parameters of the machine. For example for the cylindrical synchronous machines since  $X_d \cong X_q$ , out of synchronism occurs at zero field current when ignoring armature resistance and no-load losses.

As a summary, it should be noted that except the final equation of the maximum lagging current test, the results of all output variables like  $\delta$ ,  $E_f$ ,  $I_d$  and  $I_q$  evaluated by the present paper are different from the results presented by the previous resources for the maximum lagging current test.

#### 4 Simulation and Results

In section 3.2, a new or say modified and realistic proving procedure was presented instead of previous proof which provides better explanation and description of the maximum lagging current test. Even though the new proof seems fully correct and accurate but for much confidence, a 31.5 kVA Leroy Somer synchronous machine is simulated numerically and the simulation results are given. The test procedure is simulated exactly similar to the experimental conditions using the abc reference frame model of the machine by MATLAB/SIMULINK. Nominal values and circuit parameters of the machine which represented in Tables 1 and 2 have been extracted from the references [15] and [16]. High order space harmonics of the self and mutual inductances of the windings have been neglected when extracting the circuit parameters of the machine and its dynamic transient model. Arrays of the inductance matrix of the machine have been already calculated versus rotor position  $\theta$  precisely by the finite element method [15].

**Table 1** Nominal values of the synchronous machine.

Parameter	Unit	Value
Power	[kVA]	31.5
Line to line voltage	[V]	400
Frequency	[Hz]	50
Number of poles	-	4
Number of phases	-	3
Connection	-	Y
Per-phase resistance of the armature winding	[ $\Omega$ ]	0.199
Field winding resistance	[ $\Omega$ ]	3.7

**Table 2** Self and mutual inductances of the machine ignoring high-order space harmonics.

Inductance	Definition (H)
$L_{ff}$	2.08647
$L_{fa}(\theta)$	$0.200753095 \cos(2\theta + 1.83259581)$
$L_{aa}(\theta)$	$0.0131137837 + 0.005095737 \cos(4\theta - 2.61799383)$
$L_{ab}(\theta)$	$-0.0065160113 + 0.005770421 \cos(4\theta + 1.63704569)$

Values of the quadrature and direct-axis inductances can be evaluated using the coefficients of the inductances given in Table 2 as below [17]:

$$X_q = X_{ls} + X_{mq} = X_{ls} + \frac{3}{2} \omega_e (L_A - L_B) \quad (20)$$

$$X_d = X_{ls} + X_{md} = X_{ls} + \frac{3}{2} \omega_e (L_A + L_B) \quad (21)$$

where,  $\omega_e$  is angular frequency of the terminal voltage,  $L_A$  is the constant term of the self-inductance of the armature windings,  $L_B$  is amplitude of the sinusoidal term of the self-inductance of the armature windings and  $X_{ls}$  is leakage reactance of the armature windings which neglected in this simulation. Substituting the values of the parameters from Tables 1 and 2 into Eqs. (20) and (21), the values of 8.58 and 3.78 ohms are obtained for  $X_d$  and  $X_q$  respectively.

In order to perform the maximum lagging current test in the software environment, similar to actual conditions a small frictional load is applied to the motor. The torque of the friction load is assumed reliant on speed proportionally that its value at the rated speed is equal to 1% of the rated power of the machine.

According to the procedure described in section 2, after providing synchronism operation with a three-phase, 50 Hz, 300 volts (about 75% of the nominal voltage of the machine) grid, the field current decreases step by step with a small amount of increment. At each certain value of the field current the program is run for a relatively long period of time to reach the steady state operating condition. At each step, the final steady state values of the variables such as currents, input power, load angle, back emf and so on are stored for further processing. Field current is reduced step by step commencing from 4 amperes until -3.437 amperes which a further decrease of the field current with a relatively small amount of increment yields to a loss of synchronism operation.

Now if the program is run for -3.437 amperes, after a while it can be seen that the machine loses its synchronism and returns to synchronism again via slipping a pole. This matter can be seen clearly from the Figs. 4 and 5 which show the speed and load angle variations during the transient of the loss of synchronism respectively. According to Figs. 4 and 5, loss of synchronism is occurred at  $\delta \cong 225$  deg and during the out of synchronism operation firstly speed of the motor reduces and then after passing the transient, the motor continues working with the rated speed and very small power angle related to the friction.

Figures 6-a and 6-b illustrate reluctance power and electromagnetic power in a time interval including the moment of pole slipping respectively. Concentrating on Figs. 6-a and 6-b it can be realized easily that before occurrence of pole slipping, the electromagnetic torque is negative and acts similar to the friction load against the reluctance torque. Anyway in this condition, equilibrium of the torque is pretty conferred by the reluctance torque which holds positive value and it is considered as a driving torque keeping the machine in synchronous operating condition. This situation is continued until  $\delta \cong 225$  deg in which the reluctance torque reaches to its maximum value. In this state any further increase of the field current enhances size of the electromagnetic torque where the reluctance torque descends. Therefore the torque balance disappears, the machine decelerates and power angle increases. This oscillatory out of synchronous operation is continued for a sometime until at a load angle greater than 360 deg a new torque equilibrium and synchronous operation is established.

Figures 7 and 8 illustrate variations of the reactive power and the rms value of the lagging phase current for a time interval in which the slipping occurs. From these figures which are analogous in some way it can be realized that the maximum values of the reactive power and current do not beat the nominal values of the machine. This can be related to amplitude of the terminal voltage which has been chosen consciously as small as %75 of its nominal value.

Figures 9-a, 9-b and 9-c show the back emf and terminal voltages of phase 'a' against time for three time intervals positioned before the pole slipping, the asynchronous operation and the new synchronous operation respectively. These figures illustrate the variations of the phase angle of the back emf regarding the phase angle of the terminal voltage during the pole slipping.

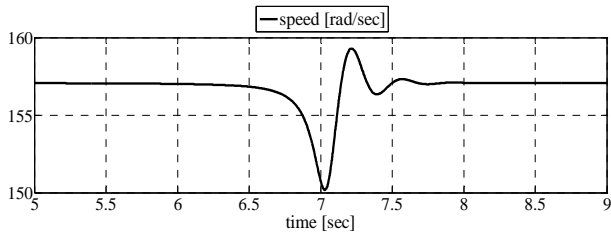


**Fig. 4** Variations of the rotor speed during pole slipping.

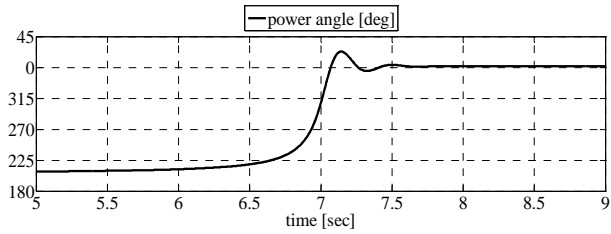


**Fig. 5** Variations of the load angle during pole slipping.

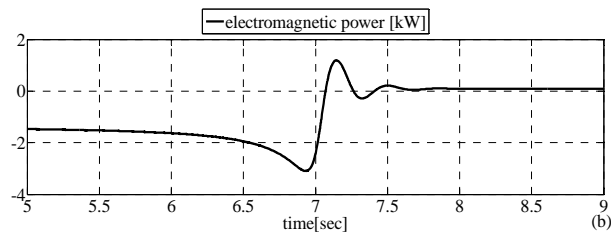
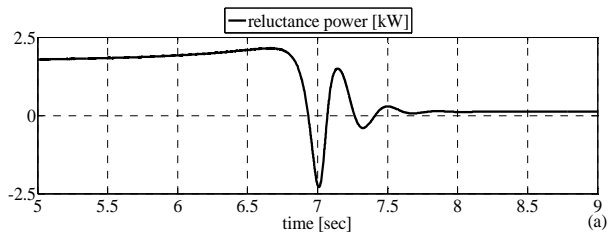


**Fig. 6** Variations of a) reluctance power and b) electromagnetic power during pole slipping.

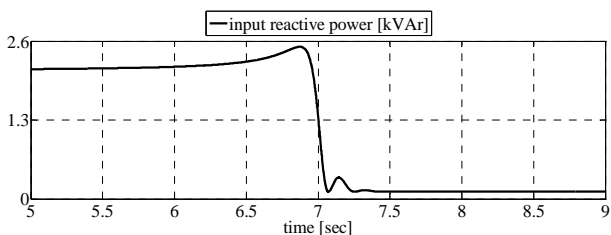


**Fig. 7** Variations of the reactive power during pole slipping.

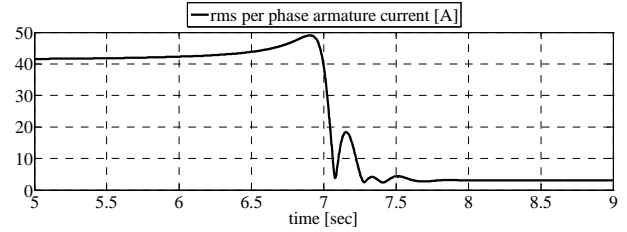


**Fig. 8** Variations of rms value of the phase current during pole slipping.

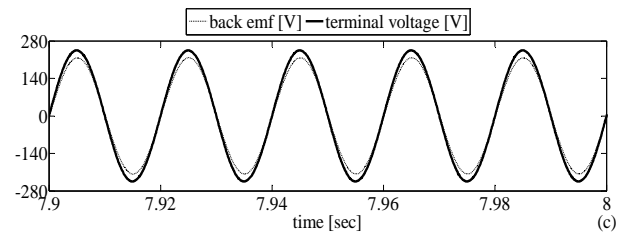
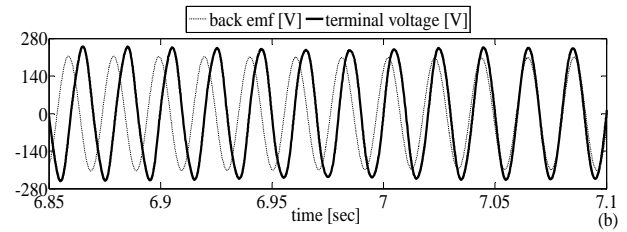
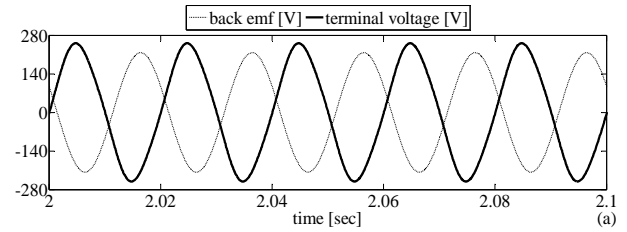


**Fig. 9** Variations of the back emf and terminal voltages a) before the pole slipping b) during the asynchronous operation and c) for the new synchronous operation.

Figures 10 and 11 show the variations of steady state back emf and power angle versus the field current respectively for the whole period of test from the beginning until pole slipping. As seen from the Fig. 11, the value of  $\delta$  is very small for the positive field current but it becomes a value greater than 180 deg just altering the direction of the field current. This angle then increases with increasing the negative field current until pole slipping occurs at about  $\delta = 225$  deg. Also the rms value of the phase current is plotted against the field current and shown in Fig. 12 for the whole period of test. This figure due to inclusion of the negative field current can be interpreted as the extended familiar V shape characteristic of the no-load motor. The maximum lagging current test is commenced with a value of the leading phase current associated with a relatively large value of the field current and then it reduces by reducing the field current until achieving a very small current at unit power factor.

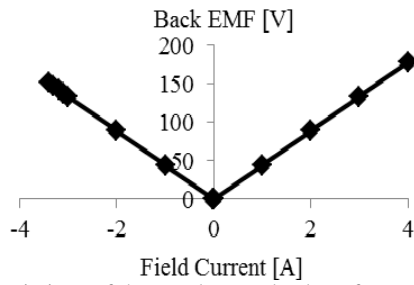


**Fig. 10** Variations of the steady state back emf versus the field current.

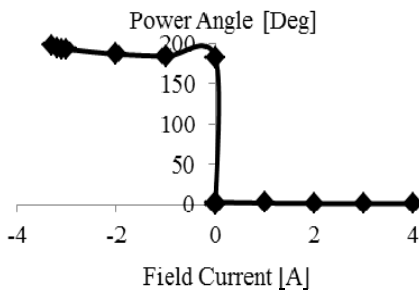


**Fig. 11** Variations of the steady state power angle versus the field current.

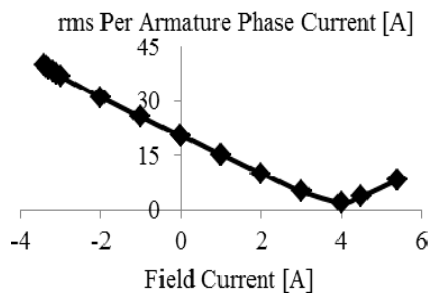


**Fig. 12** Variation of the steady state, rms value of the phase current versus the field current.

After that the phase current becomes lag and the lagging current increases by further decreasing of the field current. This situation continues by decreasing the field current to zero and then negative values until the phase current holds its maximum value and the transient out of synchronous operation occurs.

As a summary, Table 3 illustrates values of a few major variables obtained for the time nearby pole slipping occurrence by the simulation of maximum lagging current test. By substituting the values of the terminal phase voltage and current from Table 3 into the Eq. (2) quadrature-axis reactance can be achieved as follow:

$$X_q = \frac{V_t}{I_a} = \frac{173.2}{45.6} = 3.8 \text{ } [\Omega] \quad (22)$$

which the value is well-matched with the value calculated using the coefficients of the self and mutual inductance definitions written as Eq. (20) and Eq. (21).

**Table 3** Values of a few major variables recorded at the moment of pole slipping occurrence.

parameter	unit	value
$V_t$	[V]	173.2
$\delta$	[deg]	225
$\varphi$	[deg]	87.18
$E_f$	[V]	153.7
$I_a$	[A]	45.6
$I_d$	[A]	-31.39
$I_q$	[A]	-33.07
$Q$	[kVAr]	23.31

After a detail investigation given above on dynamic transient and steady state performance of the machine during maximum lagging current test, now it is a right time to conclude the discussion and aim of the present paper as below:

- 1- According to assumptions and represented analysis of subsection 3.1, pole slipping has to be occurred at  $\delta = 0 \text{ deg}$  but as seen in Table 3, the motor loses its synchronism at  $\delta = 225 \text{ deg}$  which confirms the theory introduced by the present paper in subsection 3.2.
- 2- By substituting the rms value of the terminal phase voltage and values of  $X_d$  and  $X_q$  into Eq. (8) and Eq. (17), two different values i.e. 219.93 and 155.5 volts are obtained respectively for  $E_f$  at the time of pole slipping where the later is consistent with the correct value given in Table 3. This result can be considered as the second confirmation for the proof given in the present paper.
- 3- Regarding the Fig. 1, the value of  $I_q$  should be zero at the time of pole slipping where the value of  $I_d$  is equal to  $I_a$ . However according to Table 3, the values of  $I_d$  and  $I_q$  are almost the same and equal to  $I_a/\sqrt{2}$  which validates the method of the present paper illustrated in Fig. 3. Existing small discrepancy in the values of  $I_d$  and  $I_q$  in Table 3 can be interpreted due to the small friction load which has been considered by the simulation and ignored as usual by the theory.
- 4- Regarding the theory given in section 3.2 the value of lag angle is assumed  $\varphi = 90 \text{ deg}$  at the moment of pole slipping. Therefore by applying the values of the terminal phase voltage and current from Table 3, the maximum reactive power consumed by the machine at the instant of pole slipping will be  $Q = 3V_t I_a = 23.69 \text{ kVAr}$ . This value is almost equal to the value given in Table 3 and it can be considered as another verification of the method proposed in this paper.



## 5 Conclusion

The previously published proving method of the maximum lagging current test is argued in this paper. It is shown sensibly that the proving method given for the test formula of the parameter  $X_q$  evaluation does not meet perfectly the test events of the salient pole synchronous machines. Therefore a precise proof for the maximum lagging current test is made available with all details in the current paper applying appropriate theory and discussion. For further verification of the new proof, the test routine is carefully simulated using a standard salient pole synchronous machine. Some simulation results of the test routine including dynamic transient and steady state performance of the machine are then illustrated. All the results presented in this paper validate completely the claim of the present paper. Therefore the previously published text books and standards can be revised by applying the new proving method in the future editions of the publications with some confidences.

## Acknowledgment

The work has been carried out under a contract with vice president of research and technology, University of Shahrood. The authors would like to thank its financial support.

## References

- [1] The New IEEE Standard Dictionary of Electrical and Electronics Terms (ANSI), *IEEE Std. 100-1992, 5th Revised edition*, January 15, 1993.
- [2] M. Shahnazari and A. Vahedi, "Accurate Average Value Modeling of Synchronous Machine-Rectifier System Considering Stator Resistance", *Iranian Journal of Electrical & Electronic Engineering*, Vol. 5, No. 4, pp. 253-260, Dec. 2009.
- [3] IEEE Guide for Synchronous Generator Modeling Practices in Stability Analyses, *IEEE Std. 1110-1991*, Approved March 21, 1991.
- [4] IEEE Guide for Synchronous Generator Modeling Practices and Applications in Power System Stability Analyses, *IEEE Std. 1110-2002*, 2002.
- [5] E. Da Costa Bortoni and J. Antônio Jardini, "Identification of Synchronous machine Parameters Using Load Rejection Test Data", *IEEE Trans. on Energy Conv.*, Vol. 17, No. 2, pp. 242-247, June 2002.
- [6] E. Kyriakides, G. T. Heydt and V. Vittal, "On-Line Estimation of Synchronous Generator Parameters Using a Damper Current Observer and a Graphic User Interface", *IEEE Trans. on Energy Conv.*, Vol. 19, No. 3, pp. 499-507, Sept. 2004.
- [7] A. D. Aliabad, M. Mirsalim and M. F. Aghdaei, "A Simple Analytic Method to Model and Detect Non-Uniform Air-Gaps in Synchronous Generators", *Iranian Journal of Electrical & Electronic Engineering*, Vol. 6, No. 1, pp. 29-35, March 2010.
- [8] H. Yaghobi, K. Ansari and H. Rajabi Mashhadim, "Analysis of Magnetic Flux Linkage Distribution in Salient-Pole Synchronous Generator with Different Kinds of Inter-Turn Winding Faults", *Iranian Journal of Electrical & Electronic Engineering*, Vol. 7, No. 4, pp. 260-272, Dec. 2011.
- [9] E. Da Costa Bortoni, and J. Antônio Jardini, "A Standstill Frequency Response Method for Large Salient Pole Synchronous Machines", *IEEE Trans. on Energy Conv.*, Vol. 19, No. 4, pp. 687-691, Dec. 2004.
- [10] IEEE Guide: Test Procedures for Synchronous Machines, Part I-Acceptance and Performance Testing, Part II-Test Procedures and Parameter Determination for Dynamic Analysis, *IEEE Std. 115-1995*, 1995.
- [11] IEEE Guide: Test Procedures for Synchronous Machines, *IEEE Std. 115-1983*, 1983.
- [12] P. S. Bimbhra, *Electrical machinery*, Khanna Publishers, 7th Edition, New Delhi, 2011.
- [13] N. C. Kar and A. M. El-Serafi, "Measurement of the Saturation Characteristics in the Quadrature Axis of Synchronous Machines", *IEEE Trans. Energy Conv.*, Vol. 21, No. 3, pp. 690-698, Sept. 2006.
- [14] R. Bourne, *Electrical Rotating Machine Testing*, London: Iliffe Books, pp. 114-122, 1969.
- [15] A. Hassannia, A. Darabi and M. Alshamali; "Estimation of Dynamic Parameters of a Synchronous Generator using Genetic Algorithm", *IEEJ Transactions on Electrical and Electronic Engineering*, Vol. 4, pp. 668-673, 2009.
- [16] A. Darabi; "Auxiliary Windings, Supplying the AVR of a Brushless Synchronous Generator", *Proceedings of the Eighth International Conference on Electrical Machines and Systems ICEMS 2005*, 2005.
- [17] Paul C. Krause, *Analysis of Electric Machinery and Drive Systems*, IEEE Press Publisher, Second Edition, 2002.



**Ahmad Darabi** received the B.Sc. degree from Tehran University, Tehran, Iran, in 1989 and the M.Sc. degree from the Ferdowsi University of Mashhad, Mashhad, Iran, in 1992 both in electrical engineering. He received the Ph.D. degree with the electrical machine group, Queen's University, Belfast, U.K., in 2002. He is now an associate professor and has been with Faculty of electrical and robotic engineering, University of Shahrood, Shahrood, Iran, from 1993. Also, he is head of Research Center of Electric

Propulsions, University of Shahrood, Shahrood, Iran. His research interests include design, modeling, control and manufacturing of electrical machines and generating sets.



**Mohammad Yousefifefat** was born in Minudasht, Iran in 1987. He received the B.Sc. degree in electrical engineering from the University of Mazandaran, Mazandaran, Iran, in 2010. He is currently pursuing a M.Sc. degree in the electrical engineering at University of Shahrood, Shahrood, Iran.



**Mohsen Nikkhoo** was born in Sari, Iran in 1989. He received the B.Sc. and M.Sc. degree in electrical engineering from University of Shahrood, Shahrood, Iran in 2011 and 2013 respectively. He is now cooperating with the research center of electric propulsions at University of Shahrood. His research interests include design, modelling and manufacturing of electrical machines and drive systems.